THE JOURNAL OF PHYSICAL CHEMISTRY B

Article

pubs.acs.org/JPCB

Mechanism of Solid State Amorphization of Glucose upon Milling

N. Dujardin,[†,‡] J. F. Willart,*[,†] E. Dudognon,[†] F. Danède,[†] and M. Descamps[†]

[†]Univ Lille Nord de France, F-59000 Lille, France USTL, UMET (Unité Matériaux et Transformations), UMR CNRS 8207, F-59650 Villeneuve d'Ascq, France

[‡]Université Paris-Est, CERTES, EA3481, Créteil, France

ABSTRACT: Crystalline α-glucose is known to amorphize upon milling at −15 °C while it remains structurally invariant upon milling at room temperature. We have taken advantage of this behavior to compare the microstructural evolutions of the material in both conditions in order to identify the essential microstructural features which drive the amorphization process upon milling. The investigations have been performed by differential scanning calorimetry and by powder X-ray diffraction. The results indicate that two different amorphization mechanisms occur upon milling: an amorphization at the surface of crystallites due to the mechanical shocks and a spontaneous amorphization of the crystallites as they reach a critical size, which is close to 200 Å in the particular case of α-glucose.

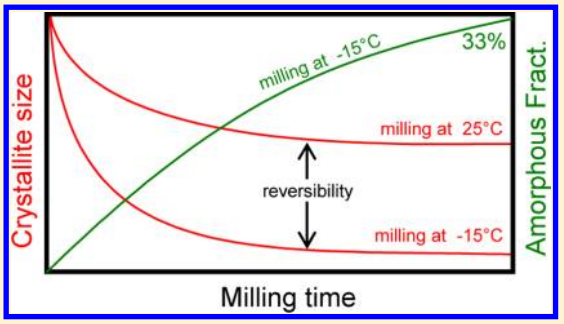

1. INTRODUCTION

Mechanical milling processes are widely used in the pharmaceutical industry as they can improve the formulation protocol and the therapeutic properties of drugs.[1] This improvement arises from two main effects: (i) Milling of a crystalline powder can strongly change its microstructural characters. In particular, it induces structural defects and leads to a size reduction of both crystallites (small single-crystals) and particles (a particle can be composed of several crystallites). These effects generally improve the solubility,[2,3] facilitate the compression of tablets,[4] and make more accurate the dosage of drugs.[5] In differential scanning calorimetry (DSC) experiments, they result in a slight decrease of both the temperature and the enthalpy of melting, while in powder X-ray diffraction (PXRD) experiments, they result in the broadening and decrease of Bragg peaks. (ii) Milling can also change the physical state itself of some crystalline materials. For instance, many solid-state amorphizations of drugs induced by milling have been reported during the past few years.[6−8] These physical changes can further improve the solubility of drugs but the intrinsic propensity of amorphous states to recrystallize generally cannot afford to guarantee the therapeutic characteristics of drugs during storage. Experimentally, such an amorphization results both in the total disappearance of Bragg peaks in PXRD patterns and in the appearance of a glass transition in heating DSC scans.

Of course, the second effect is always preceded by the first one. This means that the amorphization process induced by milling is necessarily preceded by a stage of microstructural changes. However, up to now, little is known about the exact role of the microstructural changes in the amorphization process itself. We can wonder, in particular, whether the amorphization upon milling is triggered by the strong lattice strains resulting from the many structural defects or by the crystallite size reduction or by the combination of both effects. A few papers report that the development of lattice strains due to the accumulation of defects can lead to the spontaneous amorphization of a crystalline material.[9−11] This transformation is expected to occur when the Gibbs free enthalpy of the defective crystals exceeds that of the undercooled liquid at the same temperature. A few other papers report that decreasing the size of the crystallites can also induce a spontaneous amorphization.[12,13] In that case, the amorphization is triggered by the increasing specific surface which can bring the Gibbs free enthalpy of the material above that of the corresponding undercooled liquid. This mechanism is in fact quite similar to that resulting from the defect introduction since the surface of crystallites can be considered as a bidimensional defect. The main difficulty in determining if the amorphization upon milling is triggered by the decreasing crystallite size or by the increasing defect density is clearly due to the fact that both effects occur simultaneously and are strongly correlated.

Crystalline α-glucose (G_α) ($C_6H_{12}O_6$) was recently found to amorphize (T_g = 38 °C) upon milling at −15 °C while it remains structurally invariant upon milling at room temperature (RT).[14] This change of behavior upon milling occurs in a short range of temperatures around room temperature, so that it can be easily studied by simply placing the whole milling device inside or outside a cold room at −15 °C. Several other systems are likely to show a similar behavior, but the change of behavior upon milling generally does not occur in a temperature range accessible to milling devices. Moreover, this kind of study also requires that no polymorphic transformation occurs instead of a non-amorphization process.

Received: July 12, 2012
Revised: November 19, 2012
Published: January 8, 2013

   dx.doi.org/10.1021/jp3069267 | J. Phys. Chem. B 2013, 117, 1437−1443

In this paper, we have taken advantage of this exceptional situation to compare the microstructural evolutions of this sugar in the case of an amorphization (at −15 °C) and in the case of a non-amorphization (at RT) for rigorously identical mechanical solicitations (same milling device, same mechanical solicitation). This comparison is expected to clarify how the microstructural changes trigger and govern the amorphization process upon milling. The microstructural properties of the powder (crystallite sizes and lattice strains) have been determined by a deep analysis of PXRD patterns and heating DSC scans recorded after different milling times.

2. MATERIALS AND METHODS

2.1. Sample Preparation. *Crystalline Anhydrous α-D-Glucose (G_α).* Purity ≥99.5% was purchased from Sigma Aldrich and was used without any further purification.

Ball-Milling. was performed in a high energy planetary mill (pulverizette 7 − Fritsch) at two different milling temperatures (T_{mill}): room temperature (RT ∼ 25 °C) and −15 °C. In this latter case, the whole milling device was placed in a cold room with a dehumidifier, so that the temperature can be maintained at −15 °C and 0% relative humidity. We used ZrO_2 milling jar of 45 cm^3 with seven balls (Ø = 1.5 cm) of the same material. One gram of material was placed in the planetary mill, corresponding to a ball/sample weight ratio of 75:1. The rotation speed of the solar disk was set to 300 rpm. We took care to alternate milling periods (typically 20 min.) with pause periods (typically 10 min) in order to limit the overheating of the sample.

2.2. Characterization Techniques. *Differential Scanning Calorimetry (DSC).* Experiments were performed with the TA Instruments DSC 2920 calorimeter. All the experiments have been performed with a heating rate of 5 °C/min. For all the experiments, the sample was placed in an open aluminum pan (container with no cover) and was flushed with highly pure nitrogen gas. Temperature and enthalpy readings were calibrated using pure indium at the same scan rates and with the same kind of pans used in the experiments.

Powder X-ray Diffraction (PXRD). Experiments were performed with an Inel CPS 120 diffractometer ($\lambda_{CuK\alpha}$ = 1.540 Å), equipped with a 120° curved position-sensitive detector coupled to a 4096 channel analyzer, to have a simultaneous record over 120°. Samples were placed into Lindemann glass capillaries (Ø = 0.7 mm). Analysis of the microstructure from X-ray diffraction data was then performed with the Le Bail method (using *Fullprof* software[15]).

3. RESULTS

3.1. Structural Evolution of Powders upon Milling at RT and at −15 °C. Figures 1 and 2 show the parallel evolutions of the X-ray diffraction patterns of G_α in the course of milling processes performed, respectively, at −15 °C and at RT. At −15 °C (Figure 1), the evolution is characterized by a shrinking and a strong broadening of the Bragg peaks, which finally lead to the total disappearance of Bragg peaks after 14 h of milling. This evolution reveals the amorphization of G_α upon milling at −15 °C, which has been recently reported.[14] At RT (Figure 2), the evolution is clearly different. The shrinking and the broadening of the Bragg peaks are much weaker and stop after 1 h of milling, so that after 14 h of milling, the X-ray diffraction pattern still presents well-defined Bragg peaks characteristic of the crystalline state. While broadened, these

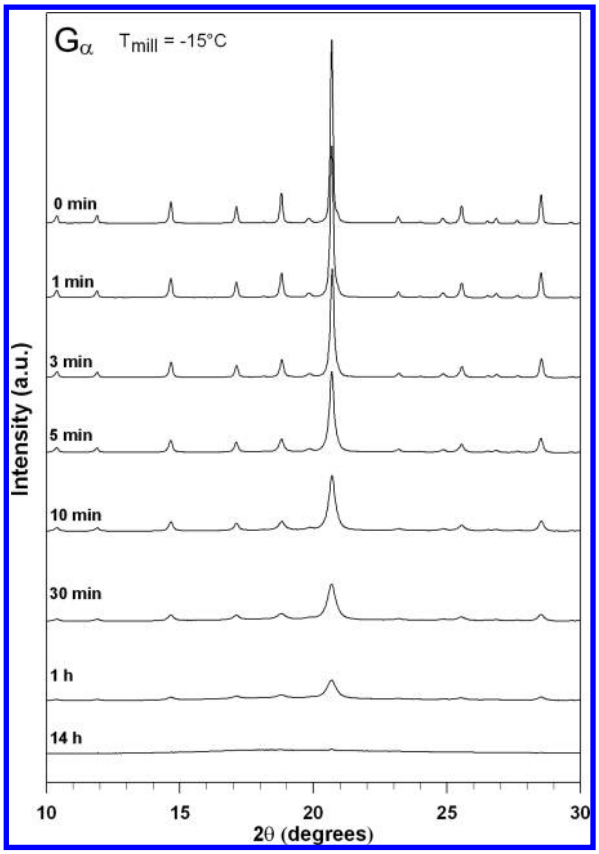

Figure 1. PXRD patterns of crystalline α-glucose upon milling at −15 °C for different milling times. The patterns have been recorded at −50 °C. The milling times are reported on the left-hand side of the figure.

Bragg peaks show integrated intensities similar to those of the unmilled G_α which indicates that the material was not amorphized by the milling process at RT. The broadening of Bragg peaks reflects the microstructural evolution of the crystalline powder during the milling process. It arises in particular from the reduction of the crystallite size and from the development of lattice strains. The constant width of Bragg peaks observed beyond 1 h of milling at RT thus reveals a stabilization of the microstructure of the crystalline powder upon milling.

Figure 3a shows the DSC heating scans (5 °C/min) of the unmilled G_α and G_α milled for 1 h at RT. While no structural transformation is induced by the milling at this temperature, the melting peaks of the two materials are noticeably different. In particular, the melting of the milled material occurs 8 °C below that of the unmilled material, and its enthalpy is decreased by 30 J/g. This evolution is known as the "Gibbs−Thomson" effect[16] and reflects the severe crystallite size reduction previously revealed by the broadening of Bragg peaks in the PXRD patterns. No further evolution of the melting peak could be detected for milling times longer than one hour suggesting—as in the case of X-ray diffraction—a stabilization of the microstructural state of the sample. The evolutions of the melting temperature and the melting enthalpy during the first hour of milling are reported in Table1.

Figure 3b shows the DSC (5 °C/min) melting peaks of samples milled 0, 1, and 29 h at −15 °C. As seen for the sample milled at RT, during the first hour of milling the melting shifts slightly toward the low temperatures and its enthalpy decreases. The temperature shift is 7 °C and the enthalpy loss is 40 J/g. It

dx.doi.org/10.1021/jp3069267 | J. Phys. Chem. B 2013, 117, 1437−1443

Figure 2. PXRD patterns of crystalline α-glucose upon milling at RT for different milling times. The patterns have been recorded at −50 °C. The milling times are reported on the left-hand side of the figure.

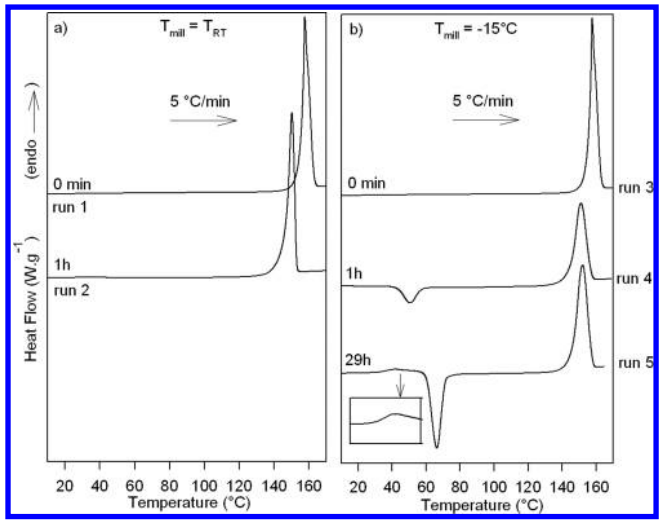

Figure 3. (a) DSC heating scans (5 °C/min) of G_α recorded after 0 h (run 1) and 1 h (run 2) of milling at RT. (b) DSC heating scans (5 °C/min) of G_α recorded after 0 h (run 3), 1 h (run 4), and 29 h (run 5) of milling at −15 °C.

must be noted that after 1 h of milling (run 4) the melting peak is preceded by a tiny C_p jump at T_g = 38 °C (midpoint of the C_p jump) and a slight recrystallization event located around 50 °C. These two features indicate that the amorphization expected upon milling at −15 °C[14] has already started during the first hour of milling. As a result, the evolution of the melting peak here not only reflects the microstructural changes in the material due to the milling, but it also takes into account the microstructure of the crystalline fraction derived from the recrystallization of the—milling induced—amorphous fraction occurring in the course of the DSC heating scan. Since this recrystallized fraction has not been milled, its melting is expected to be identical to that of the initial crystalline powder. It thus increases the apparent temperature and enthalpy of melting of the milled material. This effect is even more clearly seen for the sample milled 29 h (run 5), which appears to be totally amorphized from the amplitude of the C_p jump at T_g and from its recrystallization enthalpy. In that case, the melting only involves recrystallized material whose melting peak is very similar to that of the starting material. A slight shift of 5 °C between these two melting peaks can however be detected. It is likely due to the finely divided character of the amorphous powder obtained by milling which necessary limits the size of the crystallites produced by the recrystallization process.

Table 1. Melting Temperature (T_m) and Melting Enthalpy (ΔH_m) of Crystalline G_α Milled at RT for Different Milling Times (t_{mill})

t_{mill} (min)	T_m (±1 °C)	ΔH_m (J/g)
0	158	196 ± 2
1	157	190 ± 3
3	156	189 ± 3
5	155	173 ± 3
10	154	180 ± 3
30	151	164 ± 3
60	150	167 ± 3

The time evolution of the amorphous fraction (X_{am}) generated during the milling at −15 °C was determined from the amplitude of the C_p jump at T_g measured after different milling times. This fraction is directly given by the ratio of the C_p jump of the milled materials with that of the material milled for 29 h which has been shown to be totally amorphized (X_{am} = 1). The evolution of X_{am} during the first hour of milling at −15 °C is reported in Figure 4a. It shows that less than 1/3 of the material has been amorphized within the first hour of milling so that most of the sample requires longer milling times to be amorphized.

3.2. Microstructural Evolution of Powders upon Milling at RT and at −15 °C. The X-ray diffraction patterns of Figures 1 and 2 have been analyzed in order to determine the microstructural changes in crystalline glucose during milling at −15 °C and at RT. In particular, the changes in the crystallite sizes and in the lattice strains during the early stage of both milling processes have been determined by performing a Le Bail analysis[17] (using *Fullprof* software[15]) of the broadening of each PXRD pattern. This analysis has been performed according to the procedure described in ref 17 and using the structural parameters of crystalline glucose provided by Mcdonald and Beevers.[18,19] This method consists of a refinement of the whole diffractogram. Unlike the Rietveld method, the Le Bail analysis does not require any structural model. The intensity of the Bragg peaks is calculated by successive iterations. This procedure is based on the refinement by least-squares of calculated intensities for each data point compared to the recorded diffractogram. A pseudo-Voigt profile function with the Thompson-Cox-Hastings formalism[20] was used to fit the Bragg peaks of the X-ray patterns. This function takes into account the instrument resolution as well as the sizes and the strains of the crystallites which have a direct

dx.doi.org/10.1021/jp3069267 | J. Phys. Chem. B 2013, 117, 1437−1443

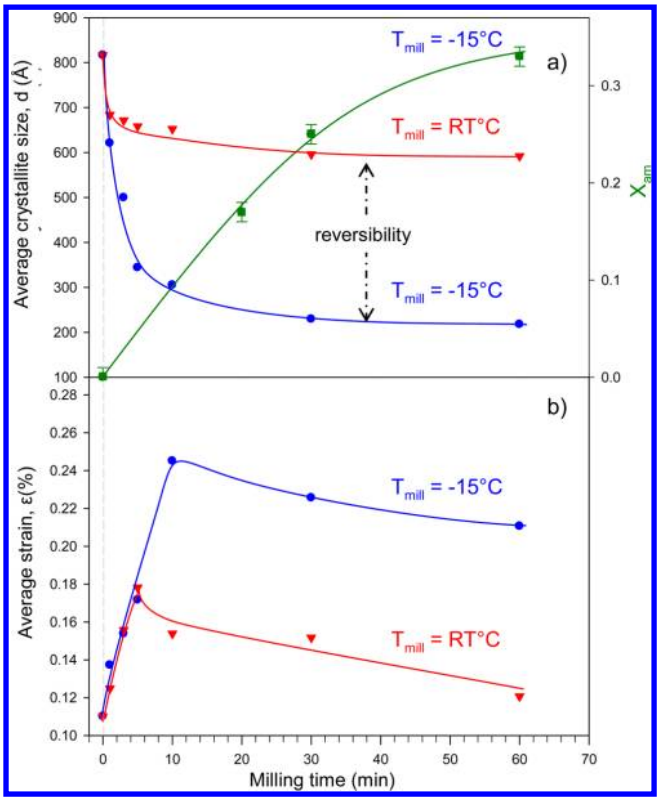

Figure 4. Time evolution of the average size d (a) and strain ε (b) of G_α crystallites upon milling at RT (▼) and at −15 °C (●), deduced from microstructural analysis (by the Le Bail method) of the PXRD patterns of Figures 1 and 2. The time evolution of the amorphized glucose fraction X_{am} determined by DSC analysis is also reported (a). The dashed arrow symbolizes the reversibility of the crystallites limit size (d_{lim}) with the milling temperature.

repercussion on the broadening of the Bragg peaks. These strains and sizes can each have an isotropic or anisotropic character. Le Bail refinements were thus performed with the four possibilities of isotropy and anisotropy. It appeared that models involving anisotropic effects do not significantly improve the fits, so that we only present here the results obtained for an isotropic modeling of both crystallite sizes and lattice strains. The normalized weighted residuals (R_{wp}) corresponding to the fits of the X-ray diffraction patterns recorded during the first hour of milling are reported in Table 2. In spite of the overlapping of neighboring Bragg peaks and the development of a diffuse background upon milling, the R_{wp} factors are found to be lower than 9%. These low values indicate[21] that all the refinements are fairly good giving confidence in the calculated microstructural parameters (size and strain). It must also be noted that the Le Bail analysis could not be performed for milling longer than one hour at −15 °C because the broadening of Bragg peaks is so strong that the fits do not converge anymore. The time evolution of the crystallite sizes and lattice strains upon milling at RT and at −15 °C are reported in Figure 4.

Table 2. Normalized Weighted Residuals (R_{wp}) Corresponding to the Le Bail Analysis of the X-ray Diffraction Patterns Recorded during the First Hour of Milling at −15°C and at RT

	R_{wp}	
milling time	T_{mill} = −15 °C	T_{mill} = RT
0 min	7.54	7.54
1 min	6.68	6.90
3 min	6.86	6.47
5 min	6.83	7.04
10 min	8.11	6.95
30 min	8.40	6.20
1 h	7.16	5.93

The evolution of the crystallite size (Figure 4a) determined during milling at RT is essentially identical to that observed during milling at −15 °C. In particular, both evolutions show an asymptotic and rapid drop of the crystallite size toward a limit size (d_{lim}). Nevertheless, this limit size is much smaller in the case of a milling at −15 °C (d_{lim} = 200 Å) than in the case of a milling at RT (d_{lim} = 600 Å). This difference of limit size cannot be due to the mechanical solicitation, which is exactly the same in both cases. It must therefore be attributed to the difference of milling temperature and to the mechanical response of the material at this temperature.

The evolutions of the deformation (Figure 4b) are also essentially identical for both milling temperatures. They can be divided in two stages. The first one is quite short and corresponds to a rapid increase of the deformations. The second stage is much longer and it corresponds to a weak decrease of these deformations. However, at −15 °C the first step is twice as long as at RT, so the deformations reach significantly higher levels during milling at −15 °C ($\varepsilon_{max}^{-15°C}$ = 0.24% ; ε_{max}^{RT} = 0.18%). Such evolutions of lattice strains have already been observed during the milling of metallic materials.[22−24] In these systems, the first step is generally attributed to a massive introduction of dislocations that pile up at grain boundaries which cannot be crossed. This rapidly causes a high increase of stresses and strains. The second step is attributed to a softening of the grain boundaries, which causes the disappearance of the dislocations and therefore a relaxation of stresses and strains in the samples. During the milling at −15 °C (Figure 4a), the glucose crystallites are quickly becoming much smaller than during the milling at RT. This gives rise to a greater total length of grain boundaries, which allows the accumulation of a much greater number of dislocations. This explains why the initial stage is longer during milling at −15 °C than at RT and why larger strains are reached. It must also be noted that many nanocrystalline materials have been found to become softer as grain size is reduced below a critical value. This so-called ″inverse Hall−Petch″ effect has mainly been observed in metallic materials by a large number of researchers,[25−27] but its origin is not yet clearly identified.

3.3. Thermodynamic Evolution of Powders Milled at RT and at −15 °C. The reduction of the average size of the crystallites induced by milling provokes a strong increase of the specific surface of the sample. This results in an excess of enthalpy in the milled samples compared to the enthalpy of the unmilled samples. As a result, the melting enthalpy of milled samples is assumed to decrease when the average crystallite size (d) decreases in the following way:[28]

$$\Delta H_m = \Delta H_m^\infty - \frac{2\gamma g V_m}{d} \quad (1)$$

where ΔH_m^∞ is the melting enthalpy of the unmilled sample, V_m the molar volume, γ the crystal/amorphous interfacial energy, and g a geometric factor which depends on the crystallite forms.

dx.doi.org/10.1021/jp3069267 | J. Phys. Chem. B 2013, 117, 1437−1443

From a thermodynamic point of view, the eq 1 predicts the existence of a critical crystallite size (d_{cr})

$$d_{cr} = \frac{2\gamma g V_m}{\Delta H_m^{\infty}} \quad (2)$$

below which the Gibbs free energy of a crystallite becomes greater than that of the amorphous grain of the same size. A spontaneous amorphization of a crystallite is thus expected when its size (d) drops below d_{cr}.

We have estimated the critical size of crystallites (d_{cr}) in the case of glucose from the melting enthalpies of samples milled from 0 to 1 h reported in Table 1. The study was only conducted for the milling at RT which produces no apparent amorphization of the sample. The melting enthalpies are thus characteristic of crystallites resulting from the mechanical fragmentation of the initial crystalline powder and not from the recrystallization of an amorphous fraction. The evolution of ΔH_m versus $1/d$ upon milling is reported in Figure 5. Despite a noticeable dispersion of points due to the rather weak enthalpy decrease generated by the fragmentation process, a linear evolution is clearly observed and can be reasonably fitted by a straight line. The extrapolation of this line to $\Delta H_m = 0$ J/g leads to a critical size of glucose crystallites close to $d_{cr} = 210 \pm 40$ Å.

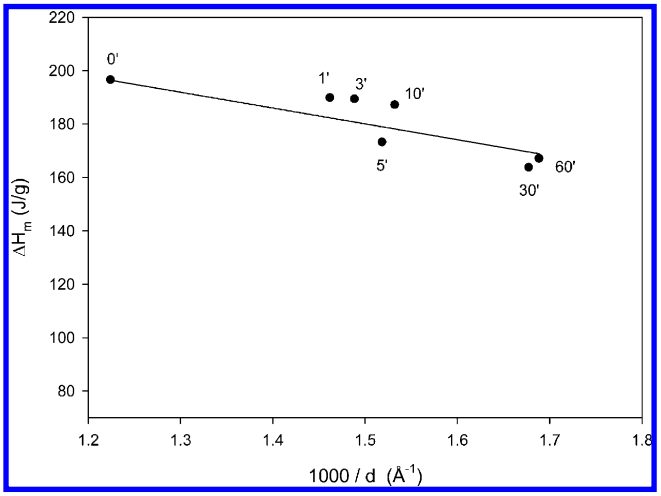

Figure 5. Enthalpy of melting of G_α after different milling times at RT versus $1/d$, where d is the crystallite size deduced from the microstructural analysis.

Below this size, the crystallites become unstable and are expected to amorphize spontaneously.

4. DISCUSSION

Changes in the microstructure of crystalline powders during milling have been extensively studied in the field of metallurgy. Some studies have shown that in the absence of structural transformation the mechanical milling leads to a stationary crystallite size resulting from a competition between a fragmentation process and a cold welding process.[29] The fragmentation arises from the high energy mechanical impacts resulting from the milling, while the cold welding is attributed to the coherent reunification of the crystallites due to the recrystallization of a small amorphous fraction generated at the impact points. We have validated this scenario in the case of glucose upon milling at RT. This was done by alternating 15 min milling stages at RT with 15 min milling stages at −15 °C. For this thermal treatment, the average crystallite size has been found to vary reversibly between $d_{lim} = 600$ Å and $d_{lim} = 200$ Å (as schematically indicated in Figure 4) which corresponds respectively to the crystallite limit sizes at RT and at −15 °C. These reversible changes with the milling temperature prove the stationary character of the crystallite size upon milling at RT and thus the existence of a competition between a mechanical fragmentation mechanism and a coherent reunification process. Moreover, it has recently been shown[14] that the milling at RT induces an effective amorphization of glucose which is, however, hardly detectable because of a much more efficient recrystallization process. This recrystallization is thus expected to be responsible for the coherent reunification of the crystallites at RT.

Upon milling at −15 °C, this recrystallization mechanism is almost nonexistent due to the very weak molecular mobility below T_g ($T_{milling} = T_g - 35$ °C). The limit size reached by the crystallites upon milling at −15 °C ($d_{lim} = 200$ Å) cannot thus result from a competition between the mechanical fragmentation mechanism and a cold welding process resulting from the recrystallization of amorphous zones located at the surface of crystallites. In addition, the limit size (d_{lim}) is reached after only one hour of milling at which time the amorphized fraction is smaller than one-half ($X_{am\ (t=1h)} < 40\%$, cf. Figure 4a). The fact that the crystallite size does not decrease anymore, while no reunification counterbalances the mechanical fragmentation, and the fact that more than half of the amorphization process

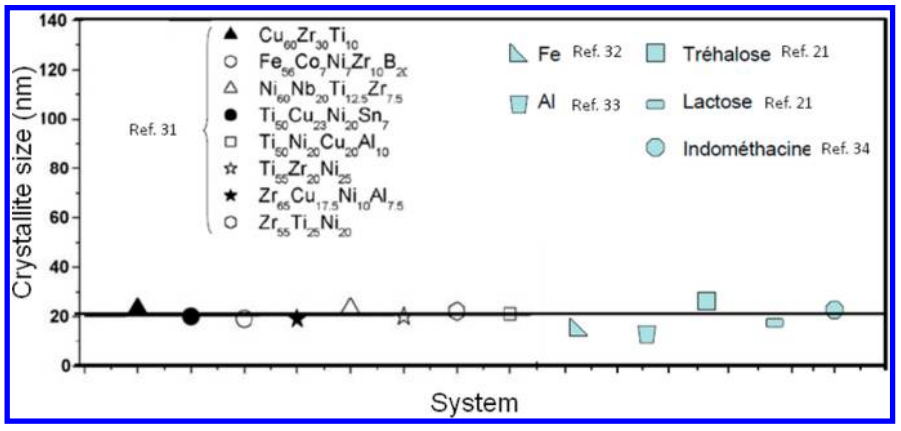

Figure 6. Critical crystallite size for different kinds of materials reported in the literature. Adapted from ref 31.

dx.doi.org/10.1021/jp3069267 | J. Phys. Chem. B 2013, 117, 1437−1443

occurs at constant crystallite size suggest that the crystallites amorphize spontaneously when their size drops below 200 Å.

The previous interpretation thus seems to be compatible with the idea of a critical size of crystallites predicted by the decreasing enthalpy of melting observed upon milling at RT (see Figure 5). For this milling temperature, the crystallite size reduction is much weaker than for the milling at −15 °C, but the lack of apparent amorphization of the milled sample allows assigning the decrease of the enthalpy of melting to the only microstructural evolution. The critical size deduced from the extrapolation of the melting enthalpy to 0 J/g is d_{cr} = 210 ± 40 Å. For this size, the surface energy of the crystallites would become greater than the volume energy so that an inversion of stability between the amorphous and crystalline states would be expected.

It appears that the critical size indirectly determined by extrapolating the heats of fusion of samples milled at RT (d_{cr} = 210 Å) is consistent with that directly determined during the amorphization process upon milling at −15 °C (d_{lim} = 200 Å). It must be noted that this agreement has been obtained for totally independent approaches which involve different analysis techniques and different milling temperatures. This reinforces, a posteriori, the coherence of the analysis as well as its interpretation. Attempts to determine a critical size of crystallites have already been performed on very different types of materials such as metal alloys,[30,31] pure metals,[32,33] or molecular materials[21,34] (cf. Figure 6). We note that, whatever the type of material, the critical sizes obtained are all between 100 and 300 Å, that is to say very close to that reported in this paper for glucose.

While the spontaneous amorphization of crystallites below a critical size can be understood from a thermodynamical point of view, it becomes puzzling when it occurs below T_g. In fact, for sub-T_g conditions the usual thermally activated molecular mobility is expected to be far too weak to achieve the long-range disordering process required to produce an amorphous solid. However, the mobility involved in the amorphization process is that of the molecules of the small crystallites obtained by fragmentation. As demonstrated by the present X-ray diffraction measurements, the corresponding size of the crystallites approaches the nanometer scale (200 Å). The mobility that has to be considered is thus that of molecules which are highly confined. The impact of the confinement of simple liquids in nanometer-sized pores on the glass transition has been reported in 1991 by Jackson and McKenna.[35] Then, a range of investigations have been performed[36] which all show that the effective T_g is strongly depressed under confinement. This means that the intermolecular cooperativity in confined geometry is lower than in the bulk and decreases with confinement size. This also leads to an effective increase of the molecular mobility which makes possible the disordering of the nanocrystals resulting from the fragmentation. It must be noted that the T_g of the amorphous end product measured by calorimetry is close to that of the bulk one. This recovered value of the bulk T_g is due to the coalescence of the amorphous nanograins upon milling and prevents the recrystallization of the amorphous milled material. Moreover, it has recently been proposed[37,38] that the milling itself could increase the molecular mobility of amorphous materials. This proposition derived from molecular dynamic simulations which have shown that steady shear deformation processes—which are typically generated upon ball milling—can provoke the recrystallization of amorphous materials. This behavior has been attributed to a so-called "driven mobility" induced by shearing and that appears to be much higher than the usual "thermally activated mobility". This driven mobility has a general character and is expected to occur in any material and for any milling temperature located below T_g. It is thus actually the main source of mobility which can best explain the spontaneous amorphization of crystallites upon milling.

5. CONCLUSION

Crystalline α-glucose is known to amorphize upon milling at −15 °C, while it remains structurally invariant upon milling at RT. We have thus taken advantage of this behavior to compare the microstructural evolutions of the material in both conditions in order to better understand the microscopic mechanisms which drive the amorphization process upon milling. The investigations have been performed during the first hour of milling by a Le Bail analysis of the PXRD patterns.

The results indicate that, whatever the milling temperature, the average crystallite size reaches a stationary value—which is close to 600 Å at RT and 200 Å at −15 °C. However, the origin of these stationary values is totally different in the two cases. At RT, the stationary crystallite size results clearly from a competition between the mechanical fragmentation of the crystallites and a—crystallographically coherent—cold welding mechanism. This cold welding is expected to be due to the recrystallization of a thin amorphous layer coating the crystallites and generated by the energetic shocks during milling. At −15 °C (T_g − 35 °C), the molecular mobility in this amorphous fraction is too weak to enable its recrystallization so that the fragmentation process is no longer counterbalanced by the cold welding mechanism. The observation of a stationary crystallite size during the amorphization process can thus only be explained by a spontaneous amorphization of the crystallites when their size drops below 200 Å. This conclusion is reinforced by an independent analysis of the melting behavior of the samples milled at RT, which predicts a thermodynamic instability of the crystallites for a critical size of crystallites close to 210 ± 40 Å.

The comparison of the microstructural evolution of α-glucose upon an amorphizing milling at −15 °C and a non-amorphizing one at RT thus gives us better insight of the amorphization process upon milling by revealing two different mechanisms: a surface amorphization due to the mechanical shocks and a spontaneous amorphization as the crystallite size reaches a critical value.

AUTHOR INFORMATION

Corresponding Author

*E-mail: jean-francois.willart@univ-lille1.fr. Tel: 33 (0)3 20 43 68 34.

Notes

The authors declare no competing financial interest.

ACKNOWLEDGMENTS

This work was supported by the Interreg IV "2 Mers Seas Zeeën" cross-border cooperation programme 2007-2013.

REFERENCES

(1) Shakhtshneider, T. P. *Mechanochemical synthesis and mechanical activation of drugs*; John Wiley and Sons: Chichester, 1999; pp 271–312.

(2) Branham, M. L.; T, M.; T, G. *Eur. J. Pharm. Sci.* **2011**, *80*, 194–202.

(3) Keck, C. M.; Müller, R. H. *Eur. J. Pharm. Sci.* **2006**, *63*, 3−16.
(4) Alderborn, G.; Nystrom, C. *Acta Pharm. Suec.* **1982**, *19*, 381−390.
(5) Clement, S.; Urutyan, H. *Chem. Eng. Prog.* **2002**, *98*, 50−54.
(6) Willart, J. F.; Descamps, M. *Mol. Pharmaceutics* **2008**, *5*, 905−920.
(7) Brittain, H. G. *J. Pharm. Sci.* **2002**, *91*, 1573−1580.
(8) Willart, J. F.; Carpentier, L.; Danède, F.; Descamps, M. *J. Pharm. Sci.* **2012**, *101*, 1570−1577.
(9) Fecht, H. J. *Nature* **1992**, *356*, 133−135.
(10) Wildfong, P. L. D.; Hancock, B. C.; Moore, M. D.; Morris, K. R. *J. Pharm. Sci.* **2006**, *95*, 2645−2656.
(11) Johnson, W. L.; Mo, L.; Krill, C. E. *J. Non-Cryst. Solids* **1993**, *156−158*, 481−492.
(12) Colombo, I.; Grassi, G.; Grassi, M. *J. Pharm. Sci.* **2009**, *98*, 3961−3986.
(13) Sun, N. X.; Lu, K. *Phys. Rev. B: Condens. Matter Mater. Phys.* **1999**, *59*, 5987−5989.
(14) Dujardin, N.; Willart, J. F.; Dudognon, E.; Hedoux, A.; Guinet, Y.; Paccou, L.; Chazallon, B.; Descamps, M. *Solid State Commun.* **2008**, *148*, 78−82.
(15) Rodriguez-Carvajal, J. *FULLPROF*, v 2.03; Clarendon Press: CEA/Saclay, France, 2003; pp 385.
(16) Keller, A.; Hikosaka, M.; Rastagi, S.; Toda, A.; Barham, P. J.; Goldbeck., G. *J. Mater. Sci.* **1994**, *29*, 2579−2604.
(17) Le Bail, A.; Duroy, H.; Fourquet, J. L. *Mater. Res. Bull.* **1988**, *23*, 447−452.
(18) McDonald, T. R. R.; Beevers, C. A. *Acta Crystallogr.* **1950**, *3*, 394−395.
(19) McDonald, T. R. R.; Beevers, C. A. *Acta Crystallogr.* **1952**, *5*, 654−659.
(20) Thompson, P.; Cox, D. E.; Hastings., J. B. *J. Appl. Crystallogr.* **1987**, *20*, 79−83.
(21) Caron, V. Mécanosynthèse et vitrification à l'état solide d'alliages moléculaires; Université des Sciences et Technologies de Lille (USTL), 2006.
(22) Koch, C. C. *Ann. Rev. Mater. Sci.* **1989**, *19*, 121−143.
(23) Cahn, R. W.; Takeyama, M.; Horton, J. A.; Liu, C. T. *J. Mater. Res.* **1991**, *6*, 57−70.
(24) Schwarz, R. B.; Koch, C. C. *Appl. Phys. Lett.* **1986**, *49*, 146−148.
(25) Carlton, C. E.; Ferreira, P. J. *Acta Mater.* **2007**, *55*, 3749−3756.
(26) Chua, B. W.; Lu, L.; Lai, M. O. *Mater. Res. Bull.* **2006**, *41*, 2102−2110.
(27) Koch, C. C.; Narayan, J. The inverse Hall-Petch effect - Fact or artifact?; Structure and Mechanical Properties of Nanophase Materials-Theory and Computer Simulations versus Experiments;Boston, MA;2001.
(28) Chen, L. C.; Spaepen, F. *Nature (London)* **1988**, *336*, 366−368.
(29) Mørup, S.; Jiang, J. Z.; Bødker, F.; Horsewell, A. *Europhys. Lett.* **2001**, *56*, 441−446.
(30) Bakker, H.; Zhou, G. F.; Yang, H. *Prog. Mater. Sci.* **1995**, *39*, 159−241.
(31) Bahtt, J.; Murty, B. S. *J. Alloy. Compd.* **2008**, *459*, 135−141.
(32) Zhao, Y. H.; Sheng, H. W.; Lu, K. *Acta Mater.* **2001**, *49*, 365−375.
(33) Okamoto, P. R.; Lam, N. Q.; Rehn, L. E. *Solid State Phys.* **1999**, *52*, 1−135.
(34) Desprez, S. Transformation de phases induites par broyage dans un composé moléculaire: l'indométhacine; Université des Sciences et Technologies de Lille, 2004.
(35) Jackson, C. L.; McKenna, G. B. *J. Non-Cryst. Solids* **1991**, *131−133*, 221−224.
(36) Jackson, C. L.; McKenna, G. B. *Chem. Mater.* **1996**, *8*, 2128−2137.
(37) Mokshin, A. V.; Barrat, J.-L. *J. Chem. Phys.* **2009**, *130*, 034502.
(38) Ilg, P.; Barrat, J. L. *Europhys. Lett.* **2007**, *79*, 26001.